Adsorption 8: 325–340, 2002


# Adsorption Kinetic Characteristics of $H_2S$ on Activated Carbon

HUNG-LUNG CHIANG
*Department of Environmental Engineering, Fooyin Institute of Technology, Kaoshsiung, Taiwan*

JIUN-HORNG TSAI AND GEN-MU CHANG
*Graduate Institute of Environmental Engineering, National Cheng Kung University, Tainan, Taiwan*

YI-CHUN HSU
*Department of Environmental Engineering and Health, Tajen Junior College of Pharmacy, En-Pu Hsiang, Pingtung Hsien, Taiwan*

*Received November 13, 2001; Revised June 27, 2002; Accepted July 5, 2002*

**Abstract.** This study compared $H_2S$ adsorption kinetic parameters in both grain adsorption and column adsorption systems. Results indicated that when the nondimensional mass transfer parameter for adsorption column design was included, the axial dispersion ($Pe > 1, \delta < 1$) and external film resistance ($B \gg 1$) could be neglected, the fluid viscosity effect was small ($Sc = 0.76$), and the adsorbate affinity was fine ($\psi$). Surface and pore diffusion controlled the adsorbent and fluid mass transfer. In addition, spent activated carbon could be treated by a thermal process and then impregnated with NaOH. After the pretreatment, the spent activated carbon could be used for $H_2S$ adsorption. Furthermore, we also propose that the $H_2S$ adsorption reaction on the carbon is due to the formation of sulfur crystals.

## Introduction

Activated carbon is widely used as an adsorbent, catalyst support and separation media (Smisek and Cerny, 1970; Bansal et al., 1988). Activated carbon can be used in pollution control to remove odor gases like $H_2S$ (Turk et al., 1989; Turk et al., 1993; Bandosz, 1999). Carbon treated with caustic materials such as KOH and NaOH have been used widely for $H_2S$ adsorption (Ikeda et al., 1988; Takeuchi et al., 1999; Lee and Reucroft, 1999). Tsai et al. (2001) detailed the reaction mechanisms of $H_2S$ adsorbed on the NaOH impregnated activated carbon.

Costa et al. (1985) investigated the internal diffusion coefficients of pure methane, ethane and ethylene as well as their binary and ternary mixtures when adsorbed on commercial activated carbon. Ikeda et al. (1988) investigated the intraparticle diffusivity of $H_2S$ adsorbed on NaOH or $Na_2CO_3$ impregnated activated carbon. The influent concentration ranged from 10 to 400 ppm while the intraparticle diffusivity was between $4.6 \times 10^{-8}$ and $2.1 \times 10^{-7}$ $m^2/s$ (Ikeda et al., 1988).

Many studies have investigated the mechanism of hydrogen sulfide oxidation over different adsorbents by oxygen at different temperatures (Steijns and Mars, 1974; Steijns et al., 1976; Ghosh and Tollefson, 1986). In general, $H_2S$ can be oxidized to form sulfur and water (Steijns and Mars, 1974; Coskun and Tollefson, 1980; Kaliva and Smith, 1983; Ghosh and Tollefson, 1986; Mikhalovsky and Zaitsev, 1997; Dalai and Tollefson, 1998). Steijns et al. (1976) indicated the sulfur of $H_2S$ oxidation product could be further oxidized to form $SO_2$ at temperatures above 200°C.

Steijns and Mars (1974) indicated $H_2S$ might be oxidized auto-catalytically when sulfur is deposited in micropores. Katoh et al. (1995) studied the oxidation mechanism of $H_2S$, methanethiol and dimethyl sulfide

mixture gases adsorbed on wet activated carbon fiber (ACF). Results indicated $H_2S$ was oxidized to form elemental sulfur in micropores and then reacted with $H_2S$ to form polysulphide ($H_2S_x$). Moreover, the polysulphide and oxygen can produce a polysulphide radical on the surface of the ACF and react with $H_2S$ to form polysulphide and $SO_2$. Steijns et al. (1976) indicated the process involves a reactionon the surface layer between the chemisorbed oxygen and the dissociatively adsorbed hydrogen sulfide. In addition, elemental sulfur formed as product of this reaction that promoted further oxidation of the $H_2S$. Mikhalovsky and Zaitsev (1997) used the XPS analyzed the $H_2S$ adsorption on activated carbon in an inert atmosphere which resulted in the formation of surface oxygen-containing complexes and elemental sulfur. Furthermore, the surface functional groups contributed significantly to the formation of $SO_2$ in $H_2S$ oxidation.

Meeyoo et al. (1998) combined adsorption and catalytic combustion to control the hydrogen sulfide emissions. Results indicated that the $H_2S$ oxidized to ionize hydrogen sulfide, which and dissolved in water that was condensed in the carbon pores from the moist gas stream at low temperature.

Bandosz and coworkers (Bandosz, 1999; Bagreev et al., 2001a, 2001b; Bagreev and Bandosz, 2001) investigated the effect of surface acidity and pH on the $H_2S$ adsorption on activated carbon and spent activated carbon. The rate-limiting step was the reaction of the adsorbed hydrogen sulfide ion with the dissociated oxygen. Heating the adsorbed $H_2S$ carbon in an air atmosphere resulted in removal of sulfur dioxide and oxidation of elemental sulfur to form sulfur oxides.

Adsorption gas separation processes are carried out in fixed bed adsorbers that contain porous adsorbent particles or pellets. The sorbent pellet is important in both external and internal mass transfer resistance. The relative differential magnitudes in varying operational conditions, inside and outside the particle, reflect the relative importance of the mass transfer parameters. Mathematical models are needed to explain the dynamics of the adsorbers in order to predict and control the separation results. Three resistances (in series) govern the gas adsorption rate: (1) Resistance to the sorbate transfer through the external gas phase surrounding the adsorbent particles, (2) Resistance to the adsorbate diffusion through the pores of the sorbent particles and, (3) Resistance corresponding to adsorption on the pore walls of the adsorbent.

In this study, the spent activated carbon, after thermal treatment and NaOH impregnation processes, was reused as an adsorbent. The mass transfer parameters in both single grain adsorption and column adsorption systems were investigated. Furthermore, we analyzed the $H_2S$ control mechanism when transferred into activated carbon.

## Theory

A film adjacent to the surface limits the rate of mass transport between a solid surface and a flowing fluid. The transport processes are represented by film coefficients that follow Fick's law (Yang, 1987):

$$Flux = k_f(C_s - C_b) \tag{1}$$

Much of the mass transfer data in packed beds have been correlated by the Ranz-Marshall equation (Noll et al., 1992):

$$\frac{2k_f \cdot r_a}{D_m} = 2.0 + 0.6\left(\frac{\mu}{\rho D_m}\right)^{1/3}(2r_a G/\mu)^{1/2}$$
$$\text{or} \quad Sh = 2.0 + 0.6Sc^{1/3}Re^{1/2} \tag{2}$$

where $Sh$, $Sc$, and $Re$ stand for the Sherwood, Schmidt, and Reynolds numbers, respectively.

The relative importance of internal and external resistance to mass transfer has been an important subject in solid-gas reactions. The Biot number expresses the ratio between internal and external gradients and has been the subject of numerous correlations in fixed bed studies. A high Biot number indicates that the major resistance is within the pellet. A typical correlation is (Yang, 1987):

$$B = \frac{0.357}{2\varepsilon_b}\frac{D_m}{D_e}Re^{0.641}Sc^{1/3} \quad \text{for } 3 < Re < 2000 \tag{3}$$

For the gas-sorbent systems of interest in gas separation, the magnitude of the Biot number is usually:

$$B \gg 1$$

Aris (1975) estimated that the mass Biot number for a packed bed was in the 5 to 500 range.

If a concentration gradient exists in a packed bed, a diffusive mass flux will occur. In addition, turbulent diffusion due to the flow also contributes to the mass flux.

Dispersion occurs in both axial and radial directions in the bed. The adsorbed bed diameter is far greater than the particle diameter. When the Peclet number is correlated with Reynolds and Schmidt numbers, one of the many empirical correlations is as follows (Yang, 1987):

$$\frac{1}{Pe} = \frac{0.3}{Re \cdot Sc} + \frac{0.5}{1 + 3.8/(Re \cdot Sc)} \quad \text{for } 0.008 < Re < 400 \quad \text{and} \quad 0.28 < Sc < 2.2 \tag{4}$$

*Macropore Diffusion*

The importance of macropore diffusion in heterogeneous catalysis macropore has made it a popular research subject. There are four kinds of macropore diffusion (1) molecular diffusion, (2) Knudsen diffusion, (3) Poiseuille flow and (4) surface diffusion. The diffusion mechanisms concern the pore structure distribution of adsorbents (Ruthven, 1984).

Mathematical relationships for each kind of macropore diffusion are shown below:

1. Molecular Diffusion.

$$D_p = \frac{D_m}{\tau} \tag{5}$$

where $Dp$ is the pore diffusivity,$Dm$ is the molecular diffusivity and $\tau$ is the tortousity factor.
Fuller et al. derived the molecular diffusivity ($Dm$) of a two-component system as follows (Bird et al., 1960; Sherwood, 1975):

$$D_m = \frac{1.0 \times 10^{-3} \times T^{1.75}}{P\left[(\Sigma\upsilon)_A^{1/3} + (\Sigma\upsilon)_B^{1/3}\right]^2}\left(\frac{1}{M_A} + \frac{1}{M_B}\right)^{1/2} \tag{6}$$

where $P$ is the total pressure, T is the absolute temperature, $(\Sigma\upsilon)_A$ and $(\Sigma\upsilon)_B$ are the molecular volumes of gases $A$ and $B$, respectively, and $M_A$ and $M_B$ are the gas molecular weights. Generally, the molecular mean free path is smaller than the pore diameter of the adsorbent. The transport mechanism is molecular diffusion.

2. Knudsen Diffusion. Knudsen showed that under these conditions the diffusivity per unit cross-sectional area of the pore is given by

$$D_k = 9700 r_p \sqrt{\frac{T}{M}} \tag{7}$$

where $D_k$, $T$ and $M$ are the Knudsen diffusivity, absolute temperature and molecular weight; respectively.

3. Poiseuille Flow. The Poiseuille flow diffusivity is shown as:

$$D_{po} = \frac{P \cdot r_p^2}{8\mu} \tag{8}$$

where $D_{po}$ is the Poiseuille diffusivity, $P_a$ is the absolute pressure,$r_p$ is the pore radius and $\mu$ is the viscosity coefficient.

4. Surface Diffusion. The overall diffusion coefficient is shown as:

$$D = D_k + \left(\frac{1 - \varepsilon_p}{\varepsilon_p}\right) \cdot KD_s \tag{9}$$

where $D$, $D_k$, $\varepsilon_p$, $K$ and $D_s$ are the overall diffusivity, Knudsen diffusivity, adsorbent porosity, equilibrium constant, and surface diffusivity.

*Micropore Diffusion*

According to Fick's law, one has:

$$N = -D_e \frac{\partial C}{\partial r} \tag{10}$$

where $N$ is the mass flux of the transferred species, $D_e$ is the effective diffusivity of the transferred species, $C$ is the concentration of transferred species, and $r$ is the distance normal to the external surface.

The micropore diffusion is derived as follows (Noll et al., 1992):

$$\frac{\partial q}{\partial t} = \frac{1}{r^2}\frac{\partial}{\partial r}\left(r^2 D_c \frac{\partial q}{\partial r}\right) \tag{11}$$

Assuming $D_c$ is constant, Eq. (11) can be derived as Eq. (12).

$$\frac{\partial q}{\partial t} = D_c\left(\frac{\partial^2 q}{\partial r^2} + \frac{2}{r}\frac{\partial q}{\partial r}\right) \tag{12}$$

The initial and boundary conditions are shown as follows:

$$q(r,0) = q_o, \quad q(r_c,t) = q_t, \left(\frac{\partial q}{\partial r}\right)_{r=0} = 0$$

then

$$\frac{\bar{q} - q_o}{q_t - q_o} = \frac{M_t}{M_\infty} = 1 - \frac{6}{\pi^2}\sum_{n=1}^{\infty}\frac{1}{n^2}\exp\left(-\frac{n^2\pi^2 D_c t}{r_c^2}\right) \tag{13}$$

and

$$\bar{q} = \frac{3}{r_c^3}\int_0^{r_c} q \cdot r^2 dr \tag{14}$$

where $q$ equals the amount adsorbed (per unit volume of sorbent), $\bar{q}$ is the average amount adsorbed in a pellet or particle, $M_\infty$ is the total mass uptake at a gas-phase concentration of $C_o$ and $M_t$ is the mass uptake at time $t$.

*Adsorption Kinetic*

Regarding transient diffusion and sorption, a mass balance on a small volume element within the grain, combined with Fick's law, gives the following differential material balance (Lin et al., 1994):

$$\varepsilon_p\frac{\partial C}{\partial t} + (1-\varepsilon_p)\rho_p \cdot \frac{\partial q}{\partial t} = \frac{\varepsilon_p}{r^\varphi}\frac{\partial}{\partial r}\left(r^\varphi D_p \frac{\partial C}{\partial r}\right) \tag{15}$$

where $\varepsilon_p$ is the adsorbent porosity, $C$ is the gas-phase concentration, $t$ is time, $\rho_p$ is the density of the adsorbent solid part, $q$ is the sorbed mass, $r$ is the sphere or cylinder radial coordinate, $\varphi$ is a shape factor equal to one for the cylindrical system and two for the spherical system (we assumed the activated carbon particle was spherical in this study and $\varphi$ equaled 2) and $D_p$ is the gas diffusivity of sorbate molecules through the intragranular pore space.

If the sorbed-phase is favored in the activated carbon system, then the first term in the equation can be discarded. The local adsorption equilibrium, following the Freundlich equation, is assumed to describe the partitioning between the gas and sorbed phases:

$$q = kC^n \tag{16}$$

where $k$ and $n$ are empirical constants.

Combining Eqs. 15 and 16 and assuming $D_p$ is constant, then

$$\frac{\partial C}{\partial t} = D_e\left(\frac{C}{C_o}\right)^{1-n} \cdot \frac{1}{r^\varphi}\frac{\partial}{\partial r}\left(r^\varphi \frac{\partial C}{\partial r}\right) \tag{17}$$

where

$$D_e = \frac{\varepsilon_p D_p}{(1-\varepsilon_p)\rho_p n k} C_o^{1-n} \tag{18}$$

is an effective diffusivity and $C_o$ is the influent concentration of adsorbate. The equation can be dimensionless as follows:

$$\frac{\partial Q}{\partial \theta} = Q^{1-n} \cdot \frac{1}{X^\varphi}\frac{\partial}{\partial X}\left(X^\varphi \frac{\partial Q}{\partial X}\right) \tag{19}$$

where $Q = \frac{C}{C_o}$, $X = \frac{r}{a}$, $\theta = \sqrt{\frac{tD_e}{a^2}}$ and $a$ is the grain or fiber radius. The appropriate initial and boundary conditions for the adsorption procedure with an external film resistance are:

$$Q(0 < X < 1, \theta = 0) = 0$$
$$\left(\frac{\partial Q}{\partial X}\right)_{X=1} = B(1 - Q_S)$$
$$\left(\frac{\partial Q}{\partial X}\right)_{(X=0,\theta)} = 0$$

For a desorption procedure, the corresponding conditions are:

$$Q(0 < X < 1, \theta = 0) = 0$$
$$\left(\frac{\partial Q}{\partial X}\right)_{X=1} = B(1 - Q_S)$$
$$\left(\frac{\partial Q}{\partial X}\right)_{(X=0,\theta)} = 0$$

where $Q_s$ represents $Q$ at the surface ($X = 1$), $B = \frac{k_f a}{D_p \varepsilon_p}$ is the Biot number of mass transfer and $k_f$ is the gas-film mass transfer coefficient. The relative mass uptake for adsorption ($\frac{M_\theta}{M_\infty}$), or the loss for desorption ($1 - \frac{M_\theta}{M_\infty}$) at a specific time can be found by integration as:

$$\left(\frac{M_\theta}{M_\infty}\right) \text{ or } \left(1 - \frac{M_\theta}{M_\infty}\right) = (\varphi + 1) \cdot \int_0^1 (X^\varphi \cdot Q_\theta)\, dX \tag{20}$$

where $M_\infty$ is the total mass uptake at a gas-phase concentration of $C_o$ and $M_\theta$ is the cumulative mass uptake at dimensionless time $\theta$.

## Experimental

This research selected original fresh activated carbon (OAC), spent activated carbon (SAC), thermally-treated spent activated carbon (TSAC), and NaOH impregnated thermally-treated spent activated carbon (NTSAC) as typical adsorbents. The activated carbons were made from coconut shell (China Activated Carbon Inc., Taiwan). SAC and TSAC were the raw materials and the intermediate products of NTSAC, respectively. OAC and NTSAC were used to investigate the $H_2S$ adsorption characteristics.

### *Original Fresh Activated Carbon (OAC)*

Original fresh activated carbon was made from coconut shell. It is produced in the manufactured process and never exposed to the polluted gas. The size of granular activated carbon was from 0.84 to 1.81 mm (average 1.0 mm).

### *Spent Activated Carbon (SAC)*

Spent activated carbon was obtained from the exhaust gas adsorption system of a petrochemical industry in southern Taiwan. It is the original fresh activated carbon that was used for gas adsorption and regenerated several times but was lost the adsorption capacity and was regarded as waste to treat by the incinerator.

### *Thermal-Treated Spent Activated Carbon (TSAC)*

50 g of SAC was placed into a vacuum oven ($10^{-1}$–$10^{-2}$ mmHg) at room temperature for 2 hrs with high purity nitrogen (99.95%). Ten g of the de-vacuumed SAC was put into another oven at 400°C for 1.5 hrs and then cooled with the high purity nitrogen to remove the adsorbed VOCs in the SAC. The thermally-treated spent activated carbon was originally a raw material of NaOH-impregnated thermally-treated spent activated carbon.

### *NaOH Impregnated Thermal-Treated Spent Activated Carbon (NTSAC)*

50 g of TSAC was placed into an oven and dried with nitrogen gas (140°C) for 6 hrs. The pretreated activated carbon was immersed in 500 mL of 1 N NaOH solution (Merck Company, Germany) and stirred for 30 minutes. Next, the immersed activated carbon was placed in a vacuum oven for 30 minutes and kept in a dryer (glass container that contained with silica gel) for 200 minutes at room temperature. Then the immersed activated carbon was filtered out from the impregnation solution and dried in an oven at 130°C for 60 hrs. Each prepared alkaline activated carbon was stored in a gas tight, nitrogen gas-filled container before use.

The pore size distribution of adsorbents was shown as Fig. 1. The pore volume sequence was TSAC $\approx$ NTSAC > OAC > SAC in pore diameters larger than 100 Å. In pore diameters less than 100 Å, the pore volume sequence was OAC > TSAC > NTSAC > SAC. Results showed the thermal-treatment process could create the pore volume for SAC. NaOH impregnated on carbon could reduce the pore volume.

### *Column Adsorption System*

An $H_2S$ simulated blend of cylinder gases was passed through a glass column 20 cm in length and 14 mm in diameter. The bottom of the adsorption column was packed with a layer of 10-cm glass beads. Five to ten grams of activated carbon (radius 0.5 mm) was packed in the column for each run. Cylinder gases of $H_2S$ (8000 ppm) were certified by suppliers (Scott Gas Company, USA). High purity nitrogen (99.95%) gas was used for the $H_2S$ dilution. No air or moisture was present in the adsorption system. The $H_2S$ influent concentrations ranged from 20–200 ppmv in the adsorption system. The flow rate, which ranged from 1.0 L/min, was controlled by a mass flow meter (Sierra Series 9000, USA).

$H_2S$ stream constituents were analyzed by a Gas Chromatograph (HP-6890) equipped with a Pulsed Flame Photometric Detector (PFPD) and chromatographic column (G.S.Q.: 30 m, ∅: 0.53 mm). The injector, column, and detector temperatures were 180, 150, and 220°C, respectively. The $H_2S$ retention time was 4.1 minutes. The $H_2S$ adsorption capacities on each activated carbon in the gas stream were analyzed by the GC/PFPD and calculated with column adsorption kinetic curves. Quality control was also conducted to ensure experimental data performance.

### *A Single Grain Adsorption System*

Gas collection tubes (500 $cm^3$) were filled with the prepared $H_2S$ gas and the pre-weighted granular activated

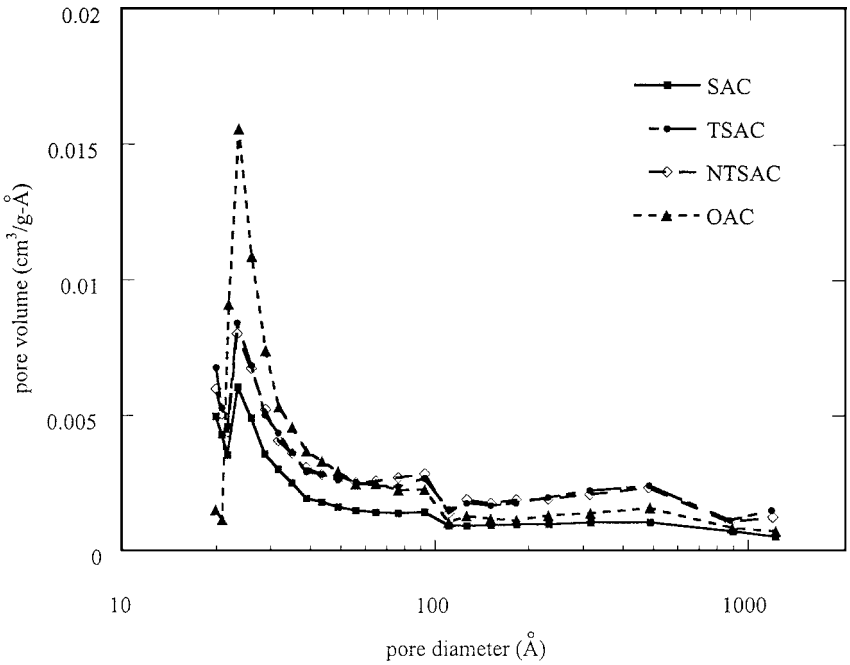


*Figure 1.* Pore size distribution of adsorbents.

carbon. Residual $H_2S$ gas from the tube was sampled with a gas syringe and analyzed for residual $H_2S$ with a GC/PFPD. The syringe took a sample (1 ml/ sample) every 10 to 20 sec for 2 min. The batch adsorption isotherm was obtained in an air-conditioned chamber ($3.0 \times 1.5$ m) at 23°C.

The particle size of the grain activated carbon was between 0.84 to 1.81 mm (average 1.0 mm). The average weight and standard deviation of the OAC and NTSAC were $1.90 \pm 0.18$ and $1.88 \pm 0.20$ mg, respectively. Non-diluted $H_2S$ gas from Scott Gas Company was used as the standard. The $r^2$, accuracy, and precision of calibration were >0.995, 95–105%, and 10%, respectively.

## Results and Discussion

In this study the adsorption mechanism of $H_2S$ on OAC and NTSAC carbons was investigated. The adsorption capacity of $H_2S$ adsorbed on activated carbon in a column adsorption system was 16–25 mg/g (concentration was 30–200 ppm), and 18–42 mg/g (concentration was 20–200 ppm) for OAC and NTSAC, respectively. In a grain adsorption system, the adsorption capacity of $H_2S$ adsorbed on activated carbon was 2.9–43.5 mg/g (concentration was 20–300 ppm), and 2.1–44.2 mg/g (concentration was 20–300 ppm) for OAC and NTSAC, respectively.

The diffusion coefficients ($D_e$, $D_s$, and $D_p$) and dimensionless parameters ($Re$, $Sc$, etc.) were measured to determine the mass transfer characteristics. The column adsorption designed parameters, external film and surface/pore diffusion, and the adsorption mechanism are interpreted in this section. The diffusion characteristics of $H_2S$ in a grain adsorption system were also investigated in this paper.

### *Mass Transfer Parameters of Column Adsorption*

The Reynolds number ($Re$), Schmidt number ($Sc$), and Sherwood number were 8, 0.76, and 5, respectively. The Schmidt number (0.76) indicated that adsorption was not affected by the viscosity of the gas phase (Tien, 1980). The Sherwood number was confirmed in literature (Yang, 1987). Results are shown in Table 1.

Results indicated the column was in a low flow rate condition; therefore, we could not neglect the effects of convection. Adsorption is a gas-solid reaction, and there is a film that can affect the transfer of adsorbate. The adsorbate transfer mechanism can be divided into two parts, the external

*Table 1.* Dimensionless parameters of $H_2S$ transferred into activated carbon in a column adsorption system.

| Dimensionless parameter | Definition | Activated carbon | | | |
|---|---|---|---|---|---|
| | | NTSAC | | | OAC |
| $R_e = \frac{Lv}{\upsilon}$ | $R_e = \frac{\text{inertial forces}}{\text{viscous forces}}$ | 8 | | | 8 |
| $Sh = \frac{Dp^2/Dm}{Dp/k_f} = \frac{2R_p k_f}{Dm}$ | $Sh = f(Sc, Re) = \frac{\text{mass transfer rate (total)}}{\text{diffusional mass transfer rate}}$ | 5 | | | 5 |
| $Sc = \frac{\upsilon}{Dm}$ | $Sc = \frac{\text{viscous transport of fluid momentum}}{\text{diffusional transport of mass}}$ | 0.76 | | | 0.76 |
| $Pe = \frac{uL}{D} = \frac{L^2/D}{L/u}$ | $\frac{\text{Time needed for dispersion}}{\text{Time needed for convection}}$ | 6 | | | 6 |
| $\delta = \frac{LDp}{uR^2}$ | Column height parameter | 0.17 | | | 0.1 |
| $\psi = kaR^2/KD_P$ | Adsorption affinity of the adsorbate | $2.3–7.0 \times 10^{-8}$ | | | $2.6–12 \times 10^{-7}$ |
| $B_i = \frac{k_f R_P}{\varepsilon_p D_p} = \frac{ShD_m}{2\varepsilon_p D_p}$ | $B_i = \frac{\text{mass transfer rate (film)}}{\text{mass transfer rate (pore)}}$ | 1885 | | | 3027 |
| | | Concentration (ppmv) | λ | Concentration (ppmv) | λ |
| $\lambda = \frac{\rho_p D_s q_{ref}}{c_{ref} D_p}$ | $\lambda = \frac{\text{surface diffusion flux}}{\text{pore diffusion flux}}$ | 21 | 1.4 | 30 | 7.0 |
| | | 65 | 0.54 | 68 | 3.8 |
| | | 105 | 0.40 | 114 | 2.6 |
| | | 174 | 0.32 | | |
| | | Concentration (ppmv) | Φ | Concentration (ppmv) | Φ |
| $\Phi = \frac{\rho_p a_p^2 G(c_{ref}, 0)}{c_{ref} D_p}$ | $\Phi = \frac{\text{rate of reaction}}{\text{rate of mass transfer}}$ | 21 | 36 | 30 | 51 |
| | | 65 | 27 | 68 | 53 |
| | | 105 | 15 | 114 | 34 |
| | | 174 | 14 | | |

film mass transfer and the internal diffusion mass transfer.

In the column adsorption system, the adsorbate was the influent in the activated carbon fixed bed. The mass transfer mechanisms included convection, axial dispersion and radial diffusion. In this column adsorption system, the Peclet number was 6 indicating the axial dispersion time was greater than the convection time. The breakthrough time could be early under a small Peclet number condition. Therefore, the Peclet number in our research indicated the adsorbate flowed perfectly into the activated carbon column. That is, the predominant mechanisms were convection and diffusion, not dispersion. Rasmuson (1981) indicated the adsorption column was displayed as a plug flow system and neglected the effect of axial dispersion when the value of $\delta < 1$. When the $\delta$ was a constant, and the Peclet number was greater than 5, the adsorption curve was similar to a Peclet number of $\infty$. When the Peclet number was $\leqq 1$, the column breakthrough time could be much earlier**.** In our research, the Peclet number was 6. The $\delta$ was 0.17 (NTSAC) and 0.10 (OAC) which demonstrated a reasonable design for our adsorption column.

When the $H_2S$ column adsorption was analyzed, the value of $\phi$ was in the vicinity of $10^{-3}$ at concentrations from 20 to 200 ppm. Increasing the influent concentration increased the value of $\phi$. Xiu (1996) showed that when the value of $\phi$ was in the vicinity of $10^{-3}$ the adsorption reaction rate was greater than the pore diffusion.

*External Film and Intraparticle Diffusion*

The adsorbate and porous activated carbon mass transfer mechanisms were included in the external film diffusion resistance and surface and pore diffusion. In order to understand the external film diffusion resistance between the adsorbate and adsorbent, we measured the NaOH Biot number; impregnated activated carbon and original activated carbon numbers were 1885 and 3027, respectively. Results indicated the rate of film mass transfer was greater than that of pore mass transfer. This may be due to the bulk solution convection flow that reduced the mass transfer resistance of the film. The NTSAC Biot number was greater than the AC number. The NaOH crystal that formed on the surface of the NTSAC could have resisted the film transfer.

*Surface and Pore Diffusion*

In other mechanisms, surface diffusion replaced adsorbate transport between the active sites. Diffusion flowed from high to low concentrations; the adsorption characteristics were temperature, adsorbate, degree of surface coverage, and energy distribution. The pore diffusion was concerned with pore size characteristics and concentration gradient distribution of the adsorbate in the pore. The NTSAC $\lambda$ value was reduced from 1.4 to 0.32 as the concentration increased from 20 to 200 ppm. Results indicated the increase in adsorbate concentration was caused by the concentration gradient increase between the external and internal adsorbent. The pore diffusion flux was also increased. In general, the surface diffusion effect can be neglected at higher influent concentrations. Surface diffusion flux was the predominant mechanism in the internal pore diffusion under low concentrations (<20 ppm). The OAC value of $\lambda$ was different than the NTSAC value. Results indicated the value of $\lambda$ was greater than 1 at all $H_2S$ concentrations. The surface diffusion flux on the OAC was larger than the pore diffusion flux at lower $H_2S$ concentrations. When the influent concentration was increased, the pore diffusion flux increased and exceeded the surface diffusion flux. The mass transfer on NTSAC was controlled by pore diffusion, and that OAC mass transfer was much more complex. At low relative vapor pressures, surface diffusion was the predominant mechanism. When the relative vapor pressure was increased the mass transfer mechanism changed from surface diffusion to pore diffusion.

Several investigators have solved governing model equations with similar boundary and initial conditions. In this research, a numerical method and Fortran least squares program were used to solve the governing equation.

The adsorption diffusivity of $H_2S$ on the NTSAC and OAC are shown in Table 2 and Fig. 2. The effective diffusivity of $H_2S$ that was adsorbed on activated carbon was between $1.4\times10^{-9}$ and $5.0\times10^{-9}$ cm$^2$/sec. When the influent concentration of $H_2S$ was from 20 ppmv to 200 ppmv on NIRAC and from 20 to 100 ppm on OAC, the effective diffusivity was between $1.4\times10^{-9}$ and $4.8\times10^{-9}$ cm$^2$/sec, and $2.7\times10^{-9}$ and $5.0\times10^{-9}$ cm$^2$/sec, respectively. The effective diffusivity was not proportional to the influent concentration. This may be due to low relative vapor pressure (from $1.01\times10^{-6}$ to $1.01\times10^{-5}$) that screened the relationship between the effective diffusivity and adsorbate concentration. The effective diffusivity on OAC was 1.5–3.0 times that of NTSAC. The NaOH crystal formation on the surface of the NTSAC may have inhibited the rate of mass transfer. The surface diffusion

*Table 2.* Diffusivity of $H_2S$ adsorbed into activated carbon.

| | Diffusion coefficient (cm$^2$/sec) | | | | | |
|---|---|---|---|---|---|---|
| Adsorbent | $De\times10^9$ | $Dm$ | $Dk\times10^3$ | $Dp\times10^4$ | $Ds\times10^{10}$ | $D\times10^3$ |
| NTSAC (A single grain adsorption) | 4160 (3000–7400) | 0.19 | 2.3 | 3900 | 9000 | 2.27 |
| OAC (A single grain adsorption system) | 2010(650–3700) | | 2.8 | 2200 | 40000 | 2.76 |
| NTSAC (Column adsorption) | 2.8 (1.4–4.8) | 0.19 | 2.3 | 5.30 | 3.8 | 2.27 |
| OAC (Column adsorption) | 4 (2.7–5.0) | | 2.8 | 3.30 | 23 | 2.76 |

$1/D = 1/D_k + 1/D_m$.
$D$: Diffusivity of transition stage.
$Dk$: Knudsen diffusivity.
$Dm$: molecular diffusivity.
$D_e = D_s + \frac{D_p}{\rho_s}\cdot\frac{\partial C}{\partial q}$.

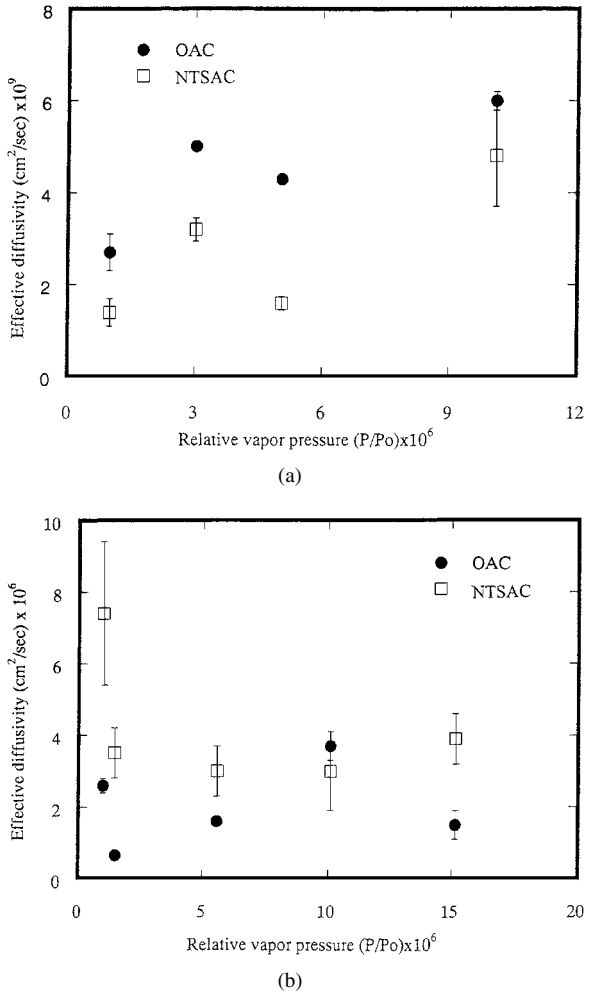


*Figure 2.* (a) Effective diffusivity of $H_2S$ into activated carbon in a column adsorption system, (b) Effective diffusivity of $H_2S$ into activated carbon in a grain adsorption system.

coefficient was 5–6 that of the pore diffusion, very slow and had significant effect on the effective diffusivity. The tourosity of NTSAC and OAC was 9 and 15, respectively, which was confirmed with the data (5–65) from literature (Ruthven, 1984). NIRAC was impregnated with NaOH to form NaOH crystals on the carbon surface to reduce the tortuosity of adsorbent. As OAC was fresh activated carbons the tortuosity of OAC was larger than NIRAC.

### *$H_2S$ Adsorption Mechanism*

The $N_2$ carrier gas experiments for $H_2S$ adsorption ($H_2S$ concentration was from 20 to 200 ppm) were carried out on the NTSAC and OAC at 25°C. This allowed the $H_2S$ adsorption kinetics to be monitored in a clean carbon surface situation. A graph of $\ln(1 - \frac{M_t}{M_e})$ versus time ($H_2S$ in the $N_2$ for adsorption at 25°C) is shown in Fig. 3. The kinetic curves could be divided into two parts by the different curve slopes. The gradient of the graph for $\frac{M_t}{M_e} < 0.7$ was less than for the region $0 < \frac{M_t}{M_e} < 0.7$. This result was similar to the study of Malik et al. (1996).

It is proposed that the apparent increase was associated with the pore-filling cooperative effects and/or the adsorption on sites of different energies at high surface coverages. Furthermore, it is proposed that the final very slow stage was associated with the reaction of $H_2S$ with the NTSAC. At low surface coverage, the $H_2S$ uptake rate is determined by the pore structure of carbon. At higher surface coverage, the adsorbed amount increased that proposed with pore filling cooperative effect. Furthermore, the $H_2S$ adsorbed and reacted with the carbon surface in the final slow stage.

In general, physical adsorption was the predominant OAC mechanism. A detailed observation of $H_2S$ adsorption at 200 ppm indicated the slope of the adsorption curve was higher than that at lower concentrations in the initial adsorption stage. The $\Phi$ value was lower than that at lower concentrations. The increase in influent concentration corresponded to the decrease of $\Phi$. This may be due to the higher $H_2S$ concentration that enhanced the chemical adsorption and absorption between $H_2S$ and NTSAC. At higher concentrations, the large amount of $H_2O$ that was formed by chemical adsorption enhanced the chemical absorption of $H_2S$ on the surface of NTSAC. The average effective diffusivity of $H_2S$ ($2.8 \times 10^{-9}$ cm$^2$/s) in NTSAC was much smaller than in water ($1.41 \times 10^{-5}$ cm$^2$/s). The adsorption rate was enhanced by the chemical absorption of $H_2S$ on the water-immersed NTSAC.

### *Adsorption Reaction*

Two adsorbents were used in this experiment, OAC (non-impregnated activated carbon) and NTSAC (NaOH impregnated thermally-treated spent activated carbon). Figure 4 shows the EDX analysis results of the initial NTSAC and $H_2S$ adsorbed NTSAC. The sulfur peak on the $H_2S$ adsorbed NTSAC was significantly higher than that on the initial NTSAC. The $H_2S$ adsorbed on NTSAC and further reacted to form sulfur on the surface of the NTSAC. The $H_2S$ adsorbed-NTSAC was desorbed with nitrogen purged at 180°C and the

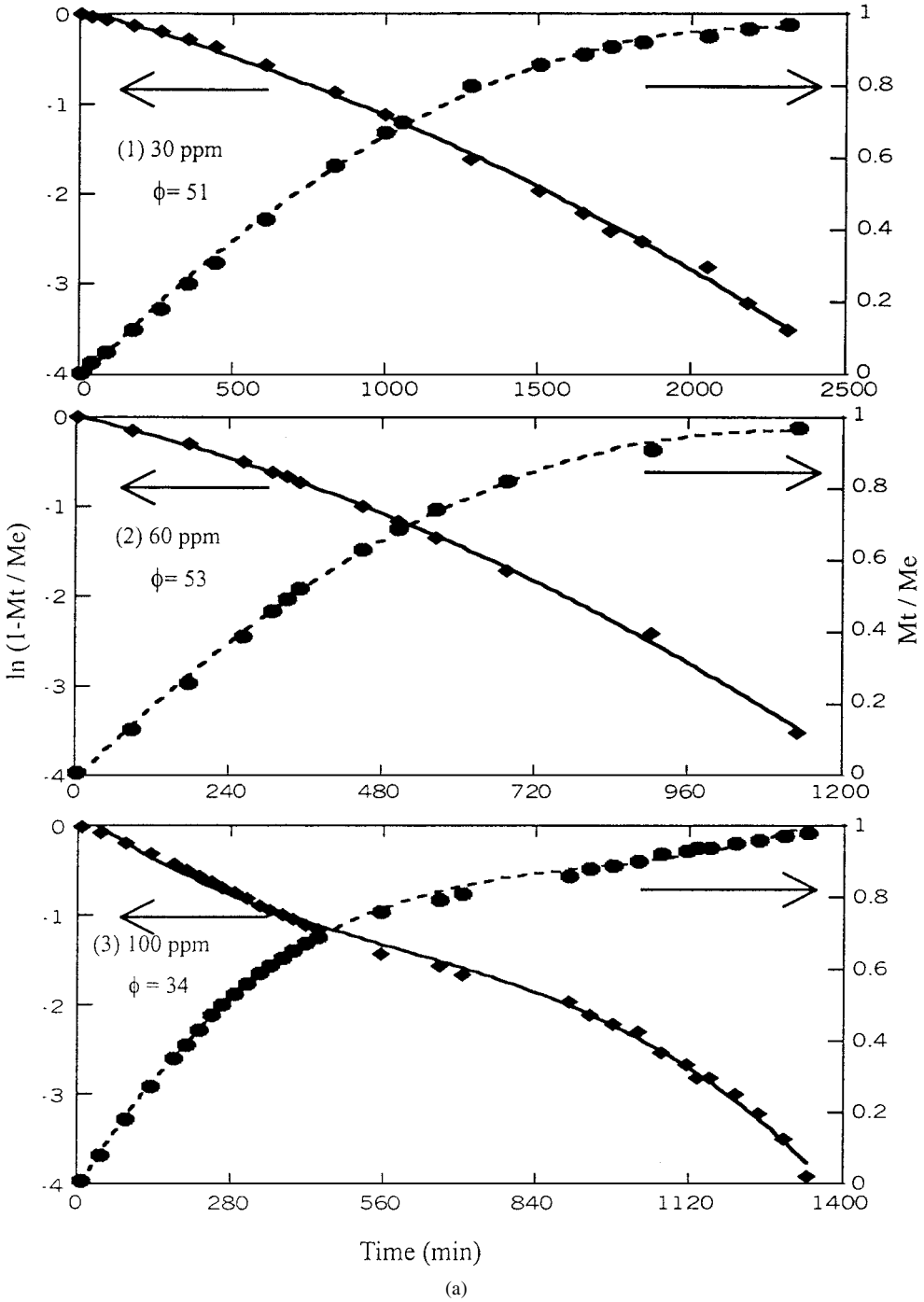


(a)

*Figure 3.* (a) Adsorption kinetic curves ($H_2S$ adsorbed into OAC) in a column adsorption system, (b) Adsorption kinetic curves ($H_2S$ adsorbed into NTSAC) in a column adsorption system.

(*Continued on next page.*)

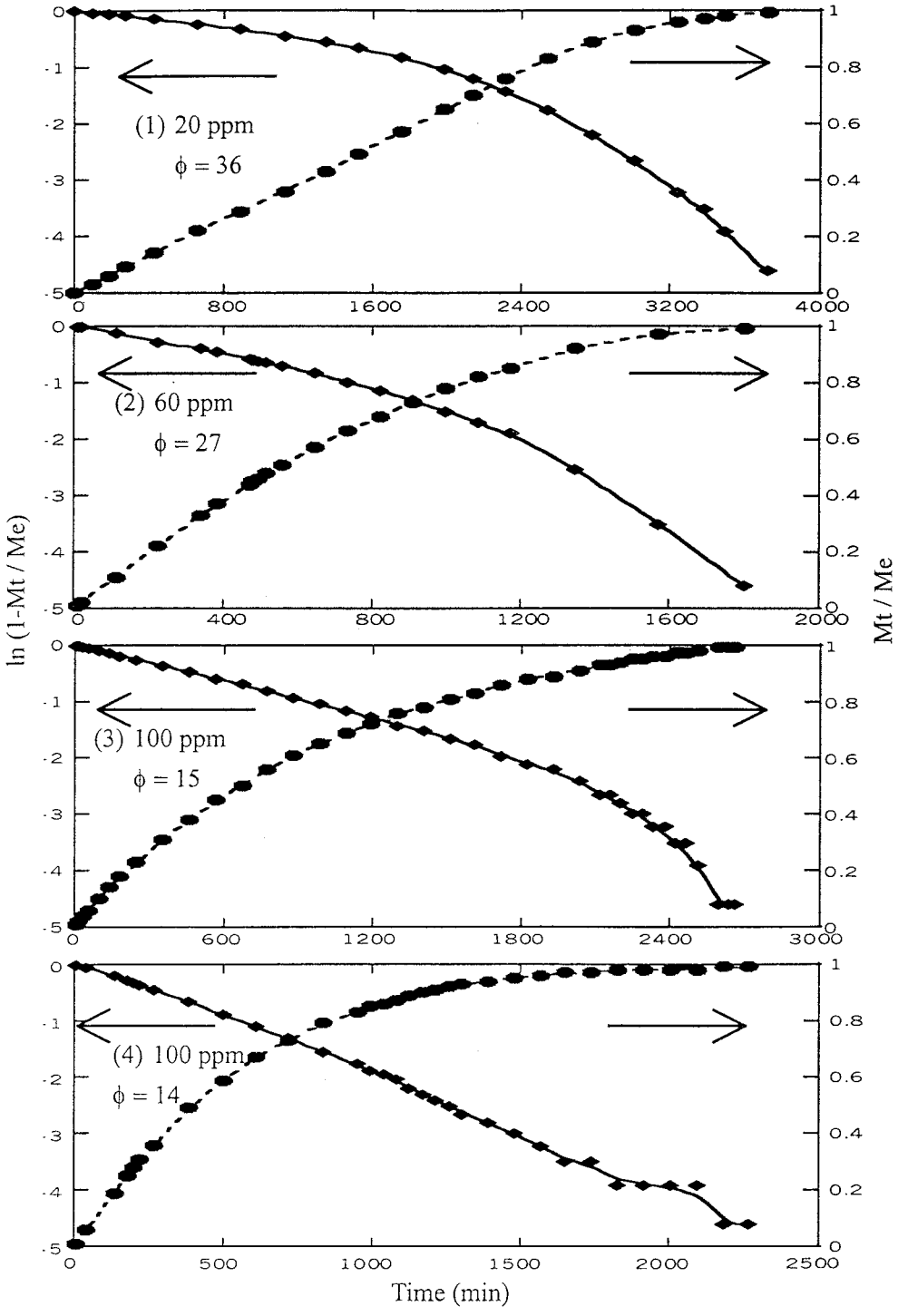


(b)

*Figure 3.* (*Continued*).

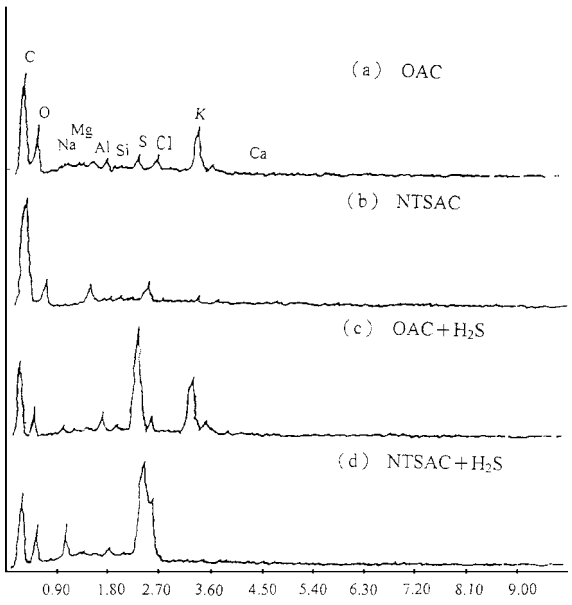


*Figure 4*. Surface element composition of carbon as analyzed by EDX analyzer.

purged gas was analyzed by GC/MS. $H_2S$ and $CS_2$ were analyzed in the desorption gas. $CS_2$ formation may be due to the sulfide compound which reacted with carbon in the high temperature desorption process.

*$H_2S$ Adsorption*

Surface analysis of the $H_2S$ adsorbed-activated carbon revealed that sulfur crystal was formed on the carbon surface. The average pore diameter of the activated carbon was 19.4 and 19.7 Å for OAC and NTSAC, respectively. In general, most activated carbon structures are similar to graphite. An activated carbon surface and pore structure is shown as Fig. 5(a). A molecular mechanical MM2 (Molecular mechanics-2) method calculated the size of the graphite pore (Burkert and Allinger, 1982). A conceptual reaction is proposed. First, the $H_2S$ transferred from the bulk stream into the pore or surface of the activated carbon (Fig. 5(b)). Figure 5(c) displays $H_2S$ adsorbed on activated carbon. The adsorbed-$H_2S$ was easily attacked by the oxidant (i.e. $O_2$, surface oxygen functional groups of activated carbon etc.) to dehydrate and form thiols structures on the carbon surface Fig. 5(d). Additionally, the nearby-thiols reacted with each other to form disulfide bonds. This reaction can be performed at low temperatures; for example, sulfur that contains amino acids can easily form an intra-disulfide bond. The nearby-disulfide further reacted to from multi-connected sulfur as shown in Fig. 5(e). Finally, a stable crown structure of $S_8$ was formed and extruded out the carbon surface Fig. 5(f). NaOH im-

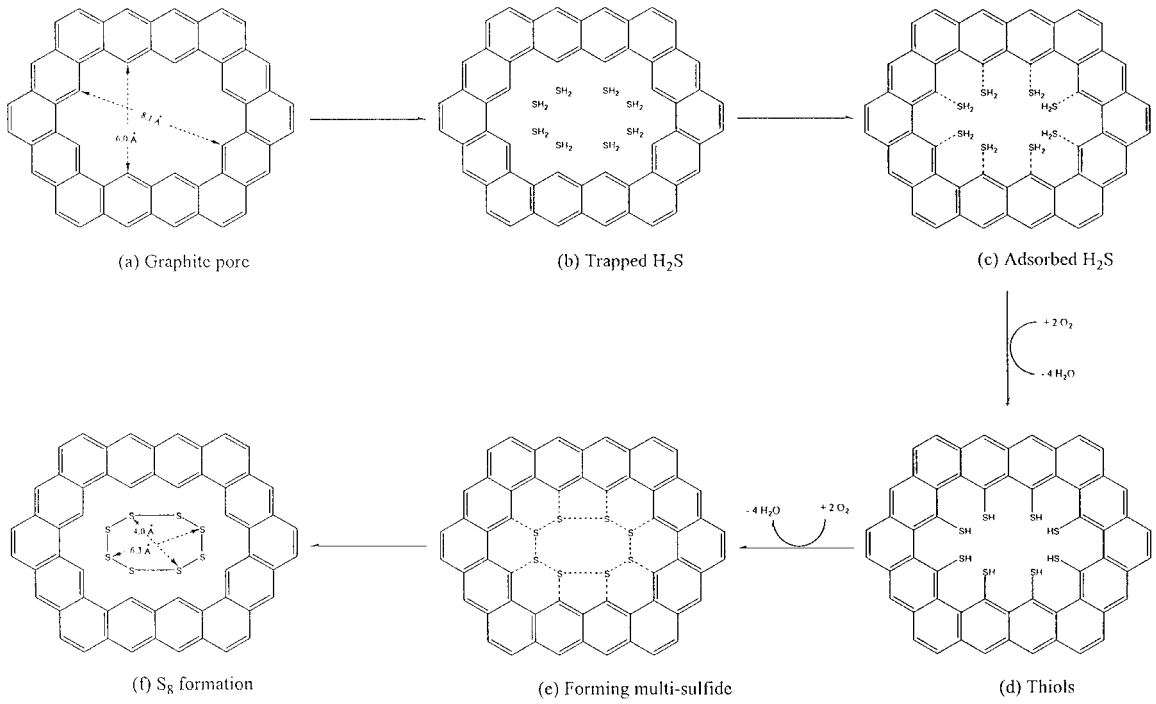


*Figure 5*. Adsorption reactions of $H_2S$ adsorbed on activated carbon.

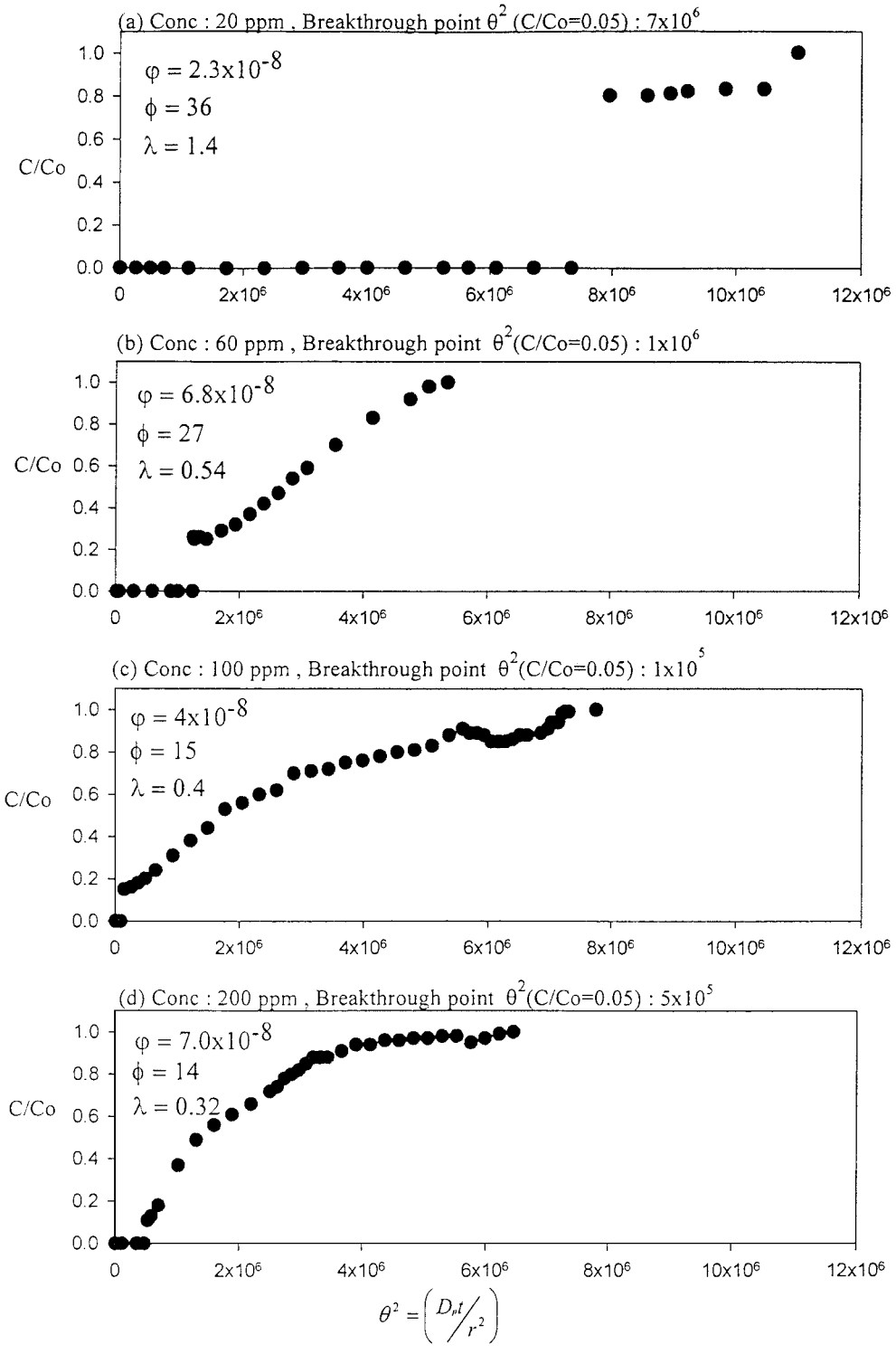


Re=8, Sc=0.76, Sh=5, Bi=1885, Pe=6, δ=0.17

*Figure 6.* Dimensionless adsorption kinetic curves of $H_2S$ (adsorbed into NTSAC) in a column adsorption system.

*Table 3*. Physical Characteristics of OAC and NTSAC.

| Adsorbent | BET surface area ($m^2$/g) | Micropore area <17 Å ($m^2$/g) | Pore volume distribution ($cm^3$/g) | | | Total pore volume ($cm^3$/g) | Pore diameter (Å) |
|---|---|---|---|---|---|---|---|
| | | | <20 Å | 20 Å < $d$ < 500 Å | >500 Å | | |
| OAC | 1143 | 990 | 0.419 | 0.091 | 0.043 | 0.553 | 19.4 |
| NTSAC | 605 | 537 | 0.170 | 0.046 | 0.016 | 0.232 | 19.7 |

pregnated on activated carbon can enhance the adsorption rate of $H_2S$. There are two possible explanations. In a dry carbon surface (lean water surface), NaOH is a base and $H_2S$ is an acid, therefore, the $H_2S$ is easily adsorbed on the carbon surface. In a wet carbon surface (rich water surface), i $H_2S$(aq) ionizes to form $HS^-$ and enhance the sorption reaction. The sulfur crystal formation reactions in this study were similar to the work of Katoh et al. (1995). In this study, we additionally investigated the effect of pore structure and explained why the sulfur crystal formed in the micropore (Fig. 5) as others have investigated (Steijns et al., 1976; Steijns and Mars, 1977; Katoh et al., 1995).

*Pore Size Distribution*

The $H_2S$ sorption mechanisms can be explained by pore size distribution and water adsorption on activated carbon. Okazaki (1978) used a two-phase equilibrium model to describe the adsorption of solvent and water vapor on activated carbon. In general, there exists only vapor-phase adsorption of organic solvents. The amount of water vapor adsorbed is negligible because the hydrophilic sites are far fewer than the hydrophobic sites on a dry surface. The $H_2S$ adsorbed on the NTSAC and reacted with NaOH to form $H_2O$. The surface of the activated carbon became hydrophilic and then the water-soluble adsorbate ($H_2S$) condensed on the $H_2O$-immersed activated carbon. Furthermore, Cal (1997) indicated that when the relative vapor pressure of water was greater than 0.5 ($\frac{p}{p_o} > 0.5$), the condensation of water vapor on a mesopore was significant. Pore size distribution of activated carbon in a macropore is >500 Å, in a mesopore, 20–500 Å, and in a micropore <20 Å. With a greater mesopore and micropore proportion, $H_2O$ is formed by the $H_2S$ and NaOH reaction that easily reacts with NaOH to form the alkali solution. Therefore, the $H_2S$ reacted with the NaOH solution like a chemical sorption system. Physical characteristics of OAC and NTSAC are shown as Table 3. The surface area and pore volume of OAC was 1.9 and 1.85 times of NTSAC, respectively.

*Adsorption Kinetic Curve*

The dimensionless parameters of $\phi$, $\Phi$, and $\lambda$ are physically defined as the affinity of adsorbate and adsorbent, the control mechanism of the adsorption process, and the adsorption control mechanism, respectively. A higher adsorbate concentration corresponds to a larger $\phi$, a smaller $\Phi$, and a smaller $\lambda$. When $\phi$ is large and $\Phi\lambda$ are small breakthrough point time ($\frac{C}{C_o} = 0.05$) is earlier and the slope of the adsorption curve is smoother. Figure 6 presents the $H_2S$ adsorption kinetic curve results.

## Conclusions

This study investigated OAC- and NTSAC- $H_2S$ adsorption. The effective diffusivity, pore diffusivity, surface diffusivity and tortousity measurements showed that internal pore diffusion was one of the predominant mechanisms of $H_2S$ adsorption on activated carbon. Surface and pore diffusion controlled the adsorption and fluid mass transfer. From this study, we propose a conceptual reaction pathway to describe the H2S that adsorbed on the carbon surface and formed sulfur crystal. This reaction pathway could explain why sulfur crystals form in the micropore.

## Nomenclature

| | |
|---|---|
| $a$ | Radius of carbon grain (cm) |
| $B$ | Biot number (dimensionless, $B = \frac{k_f a}{D_p \varepsilon_p}$) |
| $C$ | Concentration of transferred species (g/$cm^3$) |
| $C_b$ | Adsorbate concentration in the bulk stream (g/$cm^3$) |
| $Co$ | Inlet concentration of adsorbate (g/$cm^3$) |
| $C_s$ | Adsorbate concentration on the surface of adsorbent (g/$cm^3$) |
| $D$ | Overall diffusivity ($cm^2$/s) |
| $D_c$ | Crystalline diffusivity ($cm^2$/s) |
| $D_e$ | Effective diffusivity ($cm^2$/s) |
| $D_k$ | Knusen diffusivity ($cm^2$/s) |
| $D_m$ | Molecular diffusivity ($cm^2$/s) |

$D_p$ Pore diffusivity ($cm^2/s$)
$D_{po}$ Poiseuille diffusivity ($cm^2/s$)
$D_s$ Surface diffusivity ($cm^2/s$)
$D_z$ Dispersion coefficient ($cm^2/s$)
$G$ Superficial mass flux ($g/cm^2$-s)
$K$ Equilibrium constant
$k$ Empirical constant of Freundlich equation
$k_f$ The external film mass transfer coefficient (cm/s)
$M$ Molecular weight (g/mol)
$M_A$ Molecular weight of specie A (g/mol)
$M_B$ Molecular weight of specie B (g/mol)
$M_\infty$ Total mass uptake at steady state (g-adsorbate/g-adsorbent)
$M_\theta$ Cumulative mass uptake at dimensionless time $\theta$ (g-adsorbate/g-adsorbent)
$M_t$ Mass uptake at time t (g-adsorbate/g-adsorbent)
$N$ Mass flux of the transferred species ($g/cm^2$-s)
$n$ Empirical constant of Freundlich equation
$P$ Total pressure (atm)
$P_a$ Absolute pressure ($dynes/cm^2$)
$Po$ Saturated pressure (atm)
$Pe$ Pelect number (dimensionless)
$Q$ Normalized gas-phase species concentration, $C/C_o$
$Qs$ Normalized gas phase species concentration on grain surface, $X = 1$
$q$ Amount adsorbed ( per unit volume of sorbent)
$q_o$ Mass uptake at $t = 0$
$q_t$ Mass uptake at time $t$
$\bar{q}$ Average amount adsorbed in a pellet or particle
$Re$ Reynolds number ($\frac{2r_oG}{\mu}$)
$r$ Radial coordinate in carbon grain (cm)
$r_a$ Radius of adsorbent (cm)
$r_c$ Crystal radius (cm)
$r_p$ Pore radius (cm)
$Sc$ Schmit number ($\frac{\mu}{\rho D_m}$)
$Sh$ Sherwood number ($\frac{2kr_o}{D_m}$)
$T$ Absolute temperature (K)
$t$ Time (s)
$X$ Normalized radial coordinate in carbon grain, $r/a$

*Greek Letters*

$\delta$ Column height parameter (dimensionless $\frac{LDp}{uR^2}$)
$\varepsilon$ Grain porosity
$\varepsilon_b$ Interpellet void fraction in a fixed bed
$\varepsilon_p$ Adsorbent porosity
$\theta$ Dimensionless time ($\sqrt{\frac{tD_e}{a^2}}$)
$\mu$ Viscosity of gas (dyne-s/$cm^2$)
$\pi$ 3.14159
$\lambda$ Ratio of surface diffusion flux and pore diffusion flux (dimensionless, $\frac{\rho_p D_s q_{ref}}{c_{ref} D_p}$)
$\rho$ Density of stream
$\rho_p$ Density of adsorbent
$\tau$ Tortuosity (dimensionless)
$\Phi$ Ratio of reaction rate and mass transfer rate (dimensionless, $\frac{\rho_p a_p^2 G(c_{ref},0)}{c_{ref} D_p}$)
$\psi$ Adsorption affinity of the adsorbate (dimensionless, $kaR^2/KD_P$)
$(\Sigma\upsilon)_A$ Summing atomic-diffusion volume of specie $A$ ($cm^3$/mol)
$(\Sigma\upsilon)_B$ Summing atomic-diffusion volume of specie $B$ ($cm^3$/mol)
$\varphi$ Shape factor (cylindrical system = 1 and spherical system = 2)

## References


Aris, R., *Mathematical Theory of Diffusion and Reaction in Permeable Catalysts*, Vol. 1, Oxford University Press, London, 1975.

Bagreev, A., H. Rahman, and T.J. Bandosz, "Thermal Regeneration of a Spent Activated Carbon Previously Used as Hydrogen Sulfide Adsorbent," *Carbon*, **39**, 1319–1326 (2001a).

Bagreev, A., F. Adib, and T.J. Bandosz, "pH of Activated Carbon Surface as an Indication of its Suitability for $H_2S$ Removal from Moist Air Stream," *Carbon*, **39**, 1897–1905 (2001b).

Bagreev, A. and T.J. Bandosz, "$H_2S$ Adsorption/Oxidation on Unmodified Activated Carbons: Important of Prehumidification," *Carbon*, **39**, 2303–2311 (2001).

Bandosz, T.J., "Effect of Pore Structure and Surface Chemistry of Virgin Activated Carbons on Removal of Hydrogen Sulfide," *Carbon*, **37**, 483–491 (1999).

Bansal, R.C., J.B. Donnet, and F. Stoeckli, *Active Carbon*, Marcel Dekker, New York, 1988.

Bird, R.B., W.E. Stewart, and E.N. Lightfoot, *Transport Phenomena*, John Wiley and Sons, New York, 1960.

Burkert, U. and N.L. Allinger, *Molecular Mechanics*. ACS, Washington, D.C., 1982.

Cal, M.P., M.J. Rood, and S.M. Larson, "Gas Phase Adsorption of Volatile Organic Compounds and Water Vapor on Activated Carbon Cloth," *Energy & Fuel*, **11**, 311–315 (1997).

Coskun, I. and E.L. Tollefson, "Oxidation of Low Concentrations of Hydrogen Sulfide over Activated Carbon," *Can. J. Chem. Eng.* **58**, 72–76 (1980).

Costa, E., G. Calleja, and F. Domingo, "Adsorption of Gaseous Hydrocarbons on Activated Carbon: Characteristics Kinetic Curve," *AIChE*, **31**(6), 982–991 (1985).

Dalai A.K. and E.L. Tollefson, "Kinetics and Reaction Mechanism of Catalytic Oxidation of Low Concentrations of Hydrogen Sulfide

in Natural Gas over Activated Carbon" *Can. J. Chem. Eng.* **76**, 902–914 (1998).

Ghosh, T.K. and E.L. Tollefson, "Kinetics and Reaction Mechanism of Hydrogen Sulfide Oxidation over Activated Carbon in the Temperature Range of 125–200°C," *Can. J. Chem. Eng.* **64**, 969–976 (1986).

Ikeda, H., H. Asaba, and Y. Takeuchi, "Removal of $H_2S$, $CH_3SH$ and $(CH_3)_3N$ from Air by Use of Chemically Treated Activated Carbon," *J. Chem. Eng. Japan*, **21**(1), 91–97 (1988).

Kaliva, A.N. and J.W. Smith, "Oxidation of Low Concentrations of Hydrogen Sulfide by Air on a Fixed Activated Carbon Bed," *Can. J. Chem. Eng.* **61**, 208–212 (1983).

Katoh, H., I. Kuniyoshi, M. Hirai, and M. Shoda, "Studies of the Oxidation Mechanism of Sulphur-containing Gases on Wet Activated Carbon Fiber," *Applied Catalysis B: Environmental*, **6**, 255–262 (1995).

Lee, W.H. and P.J. Reucroft, "Vapor Adsorption on Coal- AND Wood-Based Chemically Activated Carbons (III) $NH_3$ and $H_2S$ Adsorption in the Low Relative Pressure Range," *Carbon*, **37**, 21–26 (1999).

Lin, T.F., J.C. Little and W.W. Nazaroff, "Transport and Sorption of Volatile Organic Compounds and Water Vapor within Dry Soil Grains," *Environ. Sci Technol*., **28**, 322–330 (1994).

Malik, A.A., P.R. Meddings, A. Patel, and K.M. Thomas, "Competitive Effects in the Adsorption of $CH_3I$ on KI-Impregnated Activated Carbon in the Presence of $CO_2$," *Carbon*, **34**, 439–447 (1996).

Meeyoo, V., J.H. Lee, D.L Trimm, and N.W. Cant, "Hydrogen Sulphide Emission Control by Combined Adsorption and Catalytic Combustion," *Catalysis Today*, **44**, 67–72 (1998).

Mikhalovsky S.V. and Y.P. Zaitsev, "Catalytic Properties of Activated Carbons I. Gas-Phase Oxidation of Hydrogen Sulfide," *Carbon*, **35**, 1367–1374 (1997).

Noll, K.E., V. Gounaris, and W.S. Hou, *Adsorption Technology for Air and Water Pollution Control*, Lewis Publishers, INC. Michigan, 1992.

Okazaki, M., H. Toman, and R. Toei, "Prediction of Binary Adsorption Equilibria of Solvent and Water Vapor on Activated Carbon," *J. Chem. Eng. of Japan*, **11**(3), 209–215 (1978).

Rasmuson, A. and I. Neretnieks, "Migration of Radionuclides in Fissured Rock the Influence of Micropore Diffusion and Longitudinal Dispersion," *J. of Geophysical Research*, **86**, 3749–3758 (1981).

Ruthven, D.M., *Principles of Adsorption & Adsorption Process*, John Wiley and Sons, New York, 1984.

Sherwood, T.K., *Mass Transfer*, McGraw-Hill, Inc., Boston, 1975.

Smisek, M. and Cerny, S., *Active Carbon*, Elsevier Science, Amsterdam, 1970.

Steijns, M. and P. Mars, "The Role of Sulfur Trapped in Micropore in the Catalytic Partial Oxidation of Hydrogen Sulfide with Oxygen," *J. of Catalysis*, **35**, 11–17 (1974).

Steijns, M., F. Derks, A. Verloop, and P. Mars, "The Mechanism of the Catalytic Oxidation of Hydrogen Sulfide," *J. of Catalysis*, **42**, 87–95 (1976).

Steijns, M. and P. Mars, "Catalytic Oxidation of Hydrogen Sulfide. Influence of Pore Structure and Chemical Composition of Various Porous Substances," *Ind. Eng. Chem., Prod. Res.*, **16**, 35–41 (1977).

Takeuchi, Y., M. Hino, Y. Yoshimura, T. Otowa, H. Izuhara, and T. Nojima, "Removal of Single Component Chlorinated Hydrocarbon Vapor by Activated Carbon of Very High Surface Area," *Sep. Puri. Tecnol*., **15**, 79–90 (1999).

Tien, C., *Adsorption Calculations and Modeling*, Butterworth-Heinemann, 1980.

Tsai, J.H., F.T. Jeng, and H.L Chiang, "Removal of $H_2S$ from Exhaust Gas by Use of Alkaline Activated Carbon," *Adsorption*, **7**(4), 357–366 (2001).

Turk, A., E. Sakalis, J. Lessuck, H. Karamitsos, and O. Rago, "Ammonia Injection Enhances Capacity of Activated Carbon for Hydrogen Sulfide and Methyl Mercaptan," *Environ. Sci. Technol*., **23**, 1242–1245 (1989).

Turk, A., K. Mahmood, and J. Mozaffari, "Activated Carbon for Air Purification in New York City's Sewage Treatment Plants," *Wat. Sci. Tech*., **27**(7/8), 121–126 (1993).

Xiu, G.H, "Modeling Breakthrough Curves in a Fixed Beds of Activated Carbon Fiber-Extract Solution and Parabolic Approximation," *Chemical Engineering Science*, **51**(16), 4039–4041 (1996).

Yang, R.T., *Gas Separation by Adsorption Processes*, Butterworth Publisher, Boston, 1987.